Order statistics of $1/f^{\alpha}$ signals

N. R. Moloney*
Max Planck Institute for the Physics of Complex Systems, Nöthnitzer Str. 38, D-01187 Dresden, Germany

K. Ozogány† and Z. Rácz‡
Institute for Theoretical Physics - HAS, Eötvös University, Pázmány sétány 1/a, H-1117 Budapest, Hungary

(Received 27 September 2011; published 1 December 2011)

Order statistics of periodic, Gaussian noise with $1/f^{\alpha}$ power spectrum is investigated. Using simulations and phenomenological arguments, we find three scaling regimes for the average gap $d_k = \langle x_k - x_{k+1} \rangle$ between the kth and $(k+1)$st largest values of the signal. The result $d_k \sim k^{-1}$, known for independent, identically distributed variables, remains valid for $0 \leqslant \alpha < 1$. Nontrivial, α-dependent scaling exponents, $d_k \sim k^{(\alpha-3)/2}$, emerge for $1 < \alpha < 5$, and, finally, α-independent scaling, $d_k \sim k$, is obtained for $\alpha > 5$. The spectra of average ordered values $\varepsilon_k = \langle x_1 - x_k \rangle \sim k^{\beta}$ is also examined. The exponent β is derived from the gap scaling as well as by relating ε_k to the density of near-extreme states. Known results for the density of near-extreme states combined with scaling suggest that $\beta(\alpha = 2) = 1/2$, $\beta(4) = 3/2$, and $\beta(\infty) = 2$ are exact values. We also show that parallels can be drawn between ε_k and the quantum mechanical spectra of a particle in power-law potentials.

DOI: 10.1103/PhysRevE.84.061101 PACS number(s): 05.40.−a, 89.75.Da, 68.35.Ct, 05.45.Tp

I. INTRODUCTION

Extreme value statistics (EVS) was first developed in mathematics [1–3]. Its importance was soon recognized and emphasized in engineering [4,5], followed by finance and environmental problems [6–10]. Although applications in physics appeared relatively late, they cover a wide range of fields, including cosmology [11,12], spin glasses [13], random fragmentation [14], percolation [15], random matrices [16], and, most actively studied at present, interface fluctuations [17–24].

The extreme value in a batch of data is important, but its study makes use of only a small fraction of the available information. Accordingly, there have been various attempts to extend studies towards near-extreme characteristics, such as the density of states near extremes [25,26], first-passage and return-time statistics [27–29], persistence [30], and record statistics [31–33]. A natural extension (which will be the concern in this paper) is to consider not only the extreme, but the sequence $x_1, x_2, \ldots, x_k, \ldots$ of the 1st, 2nd, ..., kth, ... largest, i.e., extract information from the order statistics of the system.

Order statistics has been much studied in mathematics [29,34]. All relevant quantities are known for independent, identically distributed (i.i.d.) variables, and a significant amount is also known for weakly correlated systems [29]. In physics, meanwhile, results related to order statistics are scarce: the order statistics of the brightest galaxies was recently proposed to replace the use of standard candles [35]. Another cosmological example [36] concerns an inequality satisfied by i.i.d. variables for the ratio of the average gap $\langle x_1 - x_2 \rangle$ and the standard deviation σ_1 of x_1. Violation of this inequality by the brightness data of galaxies leads to the notion that the brightest galaxies in clusters are special, in the sense that their brightness cannot simply be statistically attributed to the tail end of the luminosity distribution. An interesting example of order statistics in statistical physics concerns the positions of the k rightmost points of branching random walks [37]. The importance of this work is that it provides the exact order statistics of a system of strongly correlated particles.

For applications, it is clear that a better understanding of near-extreme properties in a correlated system is required. Here, we shall make steps in this direction by investigating the order statistics of Gaussian signals $x(t+T) = x(t)$ of period T with a $1/f^{\alpha}$ power spectrum. Depending on the value of α, such signals correspond to well-defined physical processes [white noise ($\alpha = 0$), $1/f$ noise ($\alpha = 1$), random walk ($\alpha = 2$), random acceleration ($\alpha = 4$), etc.]. As α increases, the signal changes from uncorrelated ($\alpha = 0$) to weakly correlated ($0 < \alpha < 1$), and then to strongly correlated for $1 \leqslant \alpha \leqslant \infty$. Thus, the characterization of the correlations is straightforward, and the distribution of the maximum, $x_1 = \max_t x(t) - \overline{x(t)}$, measured with respect to the time average $\overline{x(t)}$, has been discussed in the literature [19,24,38]. The present work is an extension of Ref. [24] to order statistics, and we suggest that the results may be applicable in a wide range of fields. As an example, we mention the climatic time series (of temperature, precipitation, wind speed, etc.) which appear to have correlations with the $1/f^{\alpha}$-type power spectrum, and the near-extreme properties of these quantities are clearly of much interest.

Before summarizing the results, a clarification is in order. Namely, the signal $x(t)$ is continuous for $\alpha > 1$, and thus, while the meaning of the maximum x_1 is clear, the definition of x_2 (the 2nd largest), etc., may not be obvious. The key here is to recognize that, as discussed in Sec. II, the signal is determined through a finite number of N Fourier amplitudes. The N independent values of the signal can be obtained, e.g., by sampling at equal intervals of T/N, yielding a discretized signal in which the 2nd largest, 3rd largest, etc., are well-defined.

*moloney@pks.mpg.de
†ozogany@general.elte.hu
‡racz@general.elte.hu

Our main result concerns the average gap $d_k = \langle x_k - x_{k+1} \rangle$ between the kth and $(k+1)$st largest values of the signal. We find that it scales with k as

$$d_k \sim \begin{cases} k^{-1} & \text{for} \quad 0 \leqslant \alpha < 1 \\ k^{(\alpha-3)/2} & \text{for} \quad 1 < \alpha < 5 \\ k & \text{for} \quad 5 < \alpha \leqslant \infty. \end{cases} \tag{1}$$

The above results are first obtained from simulations of the $1/f^\alpha$ signals, and then phenomenological arguments are also used to derive the exponents. As can be seen, there are three regimes, and the scaling exponents match at the borderline values $\alpha = 1$ and 5. It is suspected, however, that the power laws at $\alpha = 1$ and 5 have logarithmic corrections which are not resolved by the present simulations.

The gap scaling (1) implies that the spectrum of the average values of the kth largest behaves as

$$\varepsilon_k = \langle x_1 - x_k \rangle \sim \begin{cases} \ln k & \text{for} \quad 0 \leqslant \alpha < 1 \\ k^{(\alpha-1)/2} & \text{for} \quad 1 < \alpha < 5 \\ k^2 & \text{for} \quad 5 < \alpha \leqslant \infty. \end{cases} \tag{2}$$

The above spectrum for $1 < \alpha \leqslant \infty$ can also be obtained by relating ε_k to the density of near-extreme states which, for periodic signals, is known to be given by the distribution of the maxima of the signal relative to the initial value [26]. This distribution has been studied in detail in Ref. [26] and, in particular, the $\alpha = 2$, 4, and ∞ cases were solved exactly. Thus, provided the assumption about the scaling form $\varepsilon \sim k^\beta$ is valid, the exponents for the $\alpha = 2, 4$, and ∞ cases in Eq. (2) are exact.

Interestingly, the same spectrum (2) emerges in the quasiclassical limit of a quantum mechanical system. Namely, the energy spectrum ε_k of a particle in a one-dimensional potential $U(z) \sim |z|^\theta$ is given by $\varepsilon_k \sim k^{2\theta/(2+\theta)}$. Thus, there is a one-to-one correspondence between the exponents of the order statistics spectrum for $1 < \alpha \leqslant \infty$ and of the quantum mechanical energy spectrum for $0 < \theta \leqslant \infty$.

In order to arrive at the above results, we begin with a short introduction of $1/f^\alpha$ signals (Sec. II) followed by the description of the simplest case of $\alpha = 0$ (i.i.d. variables) in Sec. III. Numerical simulations together with scaling considerations for general α are discussed in Sec. IV. The results are rederived from the point of view of the density of near-extreme states in Sec. V, and the relationship to quasiclassical quantum spectra is presented in Sec. VI.

II. PERIODIC, GAUSSIAN $1/f^\alpha$ SIGNALS

Detailed discussions of periodic, Gaussian $1/f^\alpha$ signals and their correlation and roughness properties can be found in Refs. [24,39]. Here, we just define the relevant notation and describe how the order statistics is evaluated numerically.

The configurational weight of a Gaussian $1/f^\alpha$ signal $x(t)$ of periodicity T is given by

$$\mathcal{P}[x(t)] \propto e^{-S[x(t)]}, \tag{3}$$

where the effective action

$$S[\{c_n\};\alpha] = (2\pi)^\alpha T^{1-\alpha} \sum_{n=1}^{N/2} n^\alpha |c_n|^2 \tag{4}$$

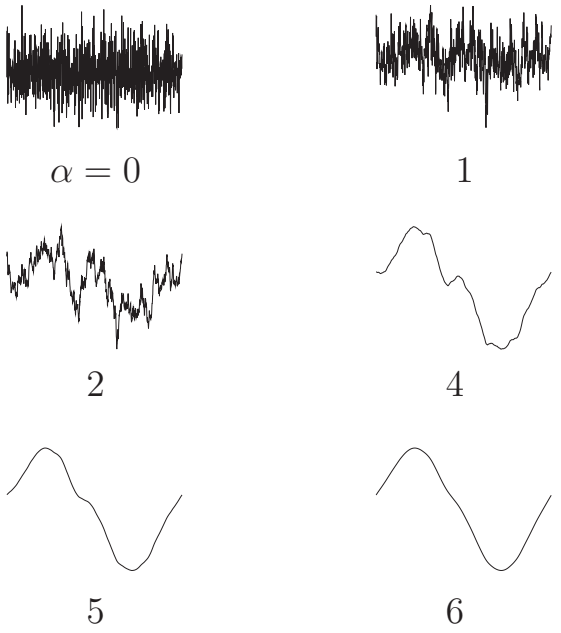

FIG. 1. Signal profiles demonstrating the increase of correlations with α (in order to emphasize the α dependence, the same random number sequence was used for generating all of the signals). The scaling regimes of the order statistics are distinct in the intervals $0 \leqslant \alpha < 1$, $1 < \alpha < 5$, and $5 < \alpha \leqslant \infty$. The borderline points ($\alpha = 1$ and 5) are associated with the changing continuity properties of the signals. They are continuous for $\alpha > 1$, while they become twice differentiable for $\alpha > 5$.

is defined through the Fourier coefficients c_n of the signal

$$x(t) = \sum_{n=-N/2+1}^{N/2} c_n e^{2\pi i n t/T}, \quad c_n^* = c_{-n}. \tag{5}$$

Here N is a positive, even integer, and the phase of c_n is drawn randomly and uniformly from the interval $[0, 2\pi]$.

From Eqs. (3) and (4) one sees that the amplitudes of the Fourier modes are independent, Gaussian distributed variables, but only for $\alpha = 0$ are they identically distributed. This is also apparent from the mean square amplitude $\langle |c_n|^2 \rangle \propto 1/n^\alpha$ which is consistent with a $1/f^\alpha$ power spectrum and independent of n only for $\alpha = 0$. Although the Fourier components c_n are uncorrelated, the corresponding time signal $x(t)$ is correlated at different times t and t' for $\alpha > 0$, and the correlation increases with increasing α (see Fig. 1). In particular, the correlation function $\langle x(t')x(t'+t) \rangle$ is bounded for $0 \leqslant \alpha < 1$ (weakly correlated regime), while it diverges for $\alpha \geqslant 1$ in the limit $T \to \infty$ with t/T finite (regime of strong correlations) [24].

The action in Eqs. (3) and (4) may be formally written in the continuum limit as

$$S[x(t)] = \frac{1}{2} \int_0^T dt \left| \frac{d^{\alpha/2} x}{dt^{\alpha/2}} \right|^2, \tag{6}$$

implying the stochastic equation of motion

$$\frac{d^{\alpha/2} x}{dt^{\alpha/2}} = \xi(t), \quad \langle \xi(t)\xi(t') \rangle = \delta(t - t'), \tag{7}$$

where $\xi(t)$ is the Gaussian white noise with a zero mean. In this form it is transparent that the signals for $\alpha = 0$, 2, and 4 describe white noise, random walk, and random acceleration, respectively. It is important to note that since the maximum frequency appearing in the sum (5) is N/T, the series does not resolve fine structure on time scales less than $\tau = T/N$. Thus, we may view the signal $x(t)$ as a batch of N variables $x_n = x(nT/N)$ $(n = 0,1,\ldots,N-1)$, and determine the order statistics by ordering the x_n. As usual in extreme statistics, we should consider the limit of the batch size going to infinity $(N \to \infty)$ and search for finite results after appropriate rescalings. In our case, the limit of the batch size going to infinity $(N \to \infty)$ is equivalent to taking the limit $T \to \infty$ with $\tau = T/N$ kept fixed.

We now describe how the order statistics is evaluated numerically. For a given α and N, the amplitude and phase of the Fourier coefficients in Eq. (5) are sampled from their (Gaussian and homogeneous, respectively) distributions, and the signal $x(t)$ is generated by a fast Fourier transform. The values $x_n = x(nT/N)$ are ordered, and the largest x_1, 2nd largest x_2, etc., are determined. The process is repeated 10^6 times in order to obtain the distribution $P_N(x_k)$, and to have well-defined averages $\langle x_k\rangle_N$, as well as gaps $d_{k,N} = \langle x_k\rangle_N - \langle x_{k+1}\rangle_N$. Signals are generated in such a way for $N = 16,32,\ldots,16384$, and the N dependence of the above quantities is examined. Finally, appropriately scaled quantities are introduced, so that a finite structure emerges in the $N \to \infty$ limit.

III. ORDER STATISTICS FOR $\alpha = 0$

We begin with the $\alpha = 0$ limit, with N i.i.d. variables drawn from a Gaussian parent distribution. The results for order statistics are known [29] in this case. In particular, the kth maximum $\langle x_k\rangle$ and its root-mean-square fluctuation $\sigma_k = \sqrt{\langle x_k^2\rangle - \langle x_k\rangle^2}$ scale for large N as

$$\langle x_k\rangle \sim \sqrt{\ln N}, \quad \sigma_k \sim 1/\sqrt{\ln N}. \tag{8}$$

The above scalings suggest that, in the $N \to \infty$ limit, finite distribution functions are obtained by introducing the scaled variable z through $x = a_N z + b_N$, where $a_N \sim 1/\sqrt{\ln N}$ and $b_N \sim \sqrt{\ln N}$. Indeed, using the "experimental" scaling $z = (x - \langle x_1\rangle)/\sigma_1$, the limit distribution $P_k(z)$ for the kth maximum is given by [29]

$$P_k(z) = \frac{1}{(k-1)!}\exp\left(-k\tilde{z} - e^{-\tilde{z}}\right), \quad \tilde{z} = az + \gamma, \tag{9}$$

where $a = \pi/\sqrt{6}$ and γ is Euler's constant.

The $P_k(z)$ distribution functions obtained from simulations of $N = 16\,384$ independent modes are displayed in Fig. 2(a) for $k = 1$ [Fisher-Tippett-Gumbel (FTG) distribution] and $k = 2$, 5, and 10. As one can see, even $N = 16\,384$ is not large enough to arrive at the limit distributions for $\alpha < 1$. This is related to the notoriously slow (logarithmic) convergence, as discussed in detail in Refs. [24,40].

Using (9) to express $\langle z_k\rangle$ via $\langle z_{k+1}\rangle$, the gap between the kth and $(k+1)$st largest is given by

$$d_k = \langle z_k\rangle - \langle z_{k+1}\rangle = \frac{1}{ak}. \tag{10}$$

The spectrum of the average values z_k can be evaluated as the sum of the gaps, and one finds for large k

$$\varepsilon_k \equiv \langle z_1\rangle - \langle z_k\rangle = \sum_{\ell=1}^{k-1} d_\ell = \frac{1}{a}\sum_{\ell=1}^{k-1}\frac{1}{\ell} \approx \frac{1}{a}\ln k. \tag{11}$$

One should note here that both the distribution $P_k(z)$ and the results for the gap and the spectrum remain valid for all parent distributions whose tail extends to infinity and decay faster than any power law (domain of attraction for the FTG universality class).

In the rest of the paper, we shall consider the case $\alpha \neq 0$ and concentrate on $P_k(z)$, d_k, and ε_k. In explaining the simulation results, we shall make use of a phenomenological argument for calculating d_k, which we demonstrate now for the i.i.d. case.

Let us assume that we are studying the order statistics in the unrescaled variable $(x_1,x_2,\ldots)$, and we discover from simulations that $\langle x_1\rangle \sim \sqrt{\ln N}$ and $\langle x_k - x_{k+1}\rangle \sim d_k/\sqrt{\ln N}$. Summing over $N/2$ gaps gives the distance from the largest to the median of the parent distribution $[\langle x_{N/2}\rangle \sim O(1)]$, such that

$$\sum_{k=1}^{N/2}\langle x_k - x_{k+1}\rangle \approx \sum_{k=1}^{N/2} d_k/\sqrt{\ln N} \approx \langle x_1\rangle \approx \sqrt{\ln N}. \tag{12}$$

Multiplying by $\sqrt{\ln N}$, the above equalities yield

$$\sum_{k=1}^{N/2} d_k \approx \ln N. \tag{13}$$

Assuming that the above sum is dominated by the d_k with a simple power-law behavior $d_k \sim k^{-\delta}$, one can read off the scaling of the gap:

$$d_k \sim k^{-1}, \tag{14}$$

in agreement with the exact expression (10).

The scaling assumption, backed up by simulations, can thus be used to develop relationships between observed quantities.

IV. ORDER STATISTICS FOR $\alpha \neq 0$

For $\alpha \neq 0$, we shall present the numerical results in the following order: First, the probability distribution P_k (Fig. 2) and, second, the N-dependent scaling of $\langle x_1\rangle$, σ_1, and $\langle x_1 - x_2\rangle$ (Fig. 3) are discussed. Then, the average gap $d_k = \langle x_k - x_{k+1}\rangle$ as a function of k (Fig. 4) is described with the N scaling removed when necessary. Finally, the spectrum ε_k is obtained by summing up the d_k.

The numerical results indicate that, depending on α, there are three distinct regimes of order statistics as we shall discuss below.

A. Weakly correlated regime ($0 < \alpha < 1$)

The distributions $P_k(z)$ obtained for $\alpha = 0.5$ [Fig. 2(b)] are characteristic of the results. As can be seen, the distributions $P_k(z)$ in Fig. 2(b) are rather close to those in Fig. 2(a). In fact, the limit distribution of the maximum x_1, in the interval $0 \leqslant \alpha < 1$, is known to be FTG distributed just as in the i.i.d. case [41]. At the same time, however, the finite-size corrections are large in this regime [24], and it is not surprising that the

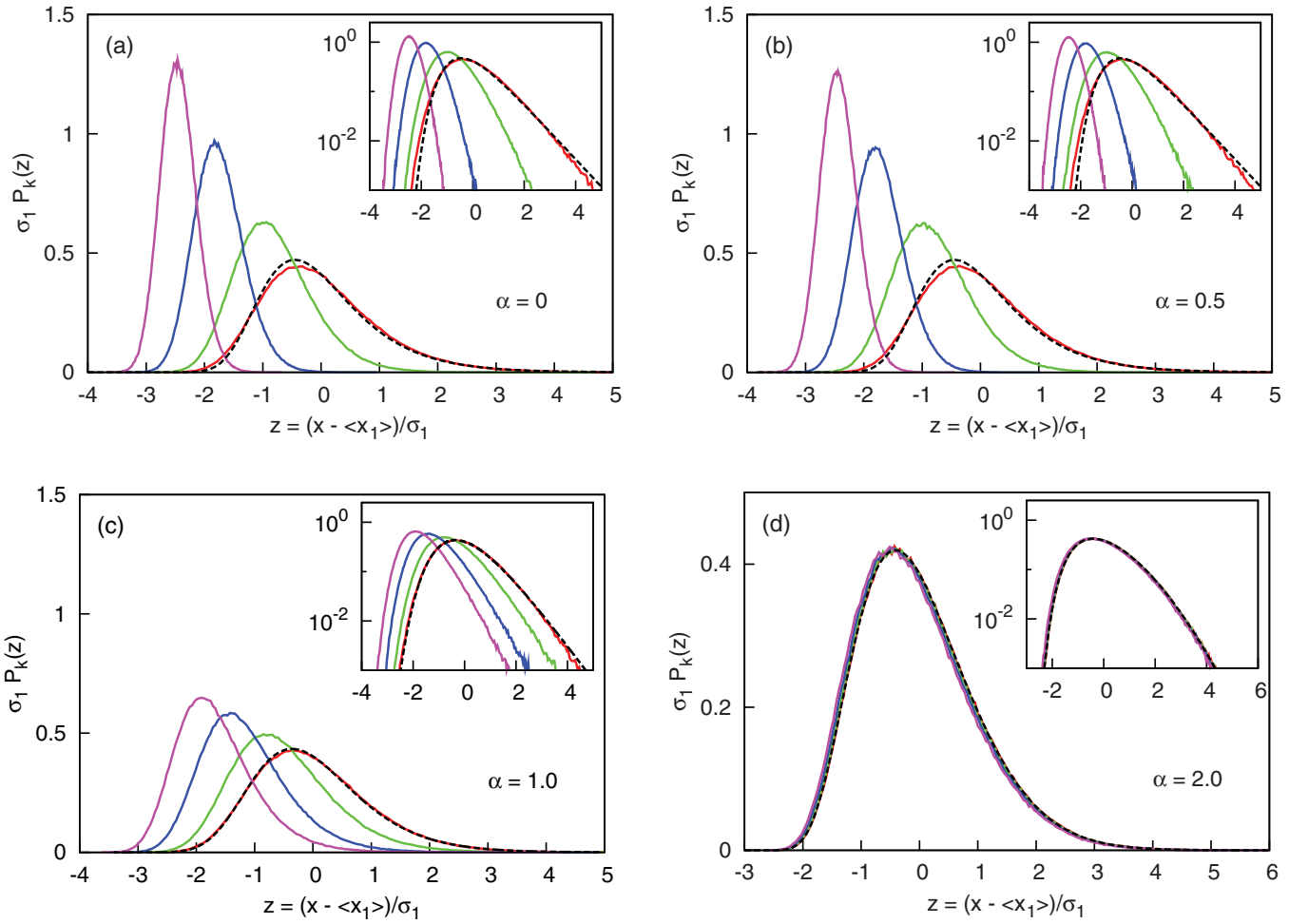

FIG. 2. (Color online) Probability distribution of the $k = 1, 2, 5$, and 10 maxima (right to left) for (a) $\alpha = 0$, (b) $\alpha = 0.5$, (c) $\alpha = 1$, and (d) $\alpha = 2$, centered and scaled according to the mean and standard deviation of the $k = 1$ maximum. Insets show the same distributions on a semilogarithmic plot. $N = 16\,384$ in all cases, and the number of simulations (10^6) is large enough so that the error bars are of the order of the width of the lines drawn. The exact limit distributions are also plotted (dashed lines) for x_1. One can see that the finite size corrections are large for $\alpha < 1$.

deviations from the limit distribution are significant even for $N = 16\,384$.

Figures 2(a) and 2(b) reveal that the widths σ_k of the distributions $P_k(x)$ are of the same order as those for $P_1(x)$, and since it is known that $\sigma_1 \sim 1/\sqrt{\ln N}$, we have $\sigma_k \sim 1/\sqrt{\ln N}$. Furthermore, the gaps $\langle x_k - x_{k+1}\rangle$ are also of the same order as σ_1, and so $\langle x_k - x_{k+1}\rangle \sim 1/\sqrt{\ln N}$. This is more precisely checked in Fig. 3, where the ratio $\langle x_1 - x_2\rangle/\sigma_1$ is plotted and, indeed, is of the order $\mathcal{O}(1)$. Similar results are obtained for all the $\langle x_k - x_{k+1}\rangle/\sigma_1$ ratios we examined ($k \leqslant 10$).

Once it is established that $\langle x_k - x_{k+1}\rangle \sim 1/\sqrt{\ln N}$, we can plot $d_k = \langle x_k - x_{k+1}\rangle\sqrt{\ln N}$ as a function of k to examine the scaling properties of the gap d_k. As Fig. 4 shows, $d_k \sim k^{-1}$, in agreement with the expectation that the weak correlations in the $0 < \alpha < 1$ regime do not affect the extreme statistics properties of the signal as compared to the i.i.d. case.

It should be noted that the $\langle x_k - x_{k+1}\rangle \approx d_k/\sqrt{\ln N}$ scaling in conjunction with the mathematical result $\langle x_1\rangle \sim \sqrt{\ln N}$ allows one to repeat the phenomenological argument given in Sec. III [see Eqs. (12)–(14)] to establish that $d_k \sim k^{-1}$ and $\varepsilon_k \sim \ln k$ (11), valid in the large k limit.

B. Regime of nontrivial scaling ($1 \leqslant \alpha < 5$)

For $\alpha \geqslant 1$, we enter the strongly correlated regime where fluctuations diverge with system size. The large-fluctuation regime can be further divided according to whether the second derivative of the signal (playing an important role in determining the order statistics) is continuous ($5 \leqslant \alpha \leqslant \infty$) or not ($1 \leqslant \alpha < 5$). Section IV B will be devoted to $1 \leqslant \alpha < 5$.

We begin with the borderline case ($\alpha = 1$) separating the weakly and strongly correlated regimes. The histograms are plotted in Fig. 2(c) and, compared to $\alpha < 1$, they draw closer to each other both in terms of location and scale. Since the $\alpha = 1$ case lies at the threshold between the two different scaling regimes for $\alpha < 1$ and $\alpha > 1$, the full quantitative details are difficult to extract. There are, however, some exact results for x_1: the first maxima scales with N as $\langle x_1\rangle \sim \ln N$, and,

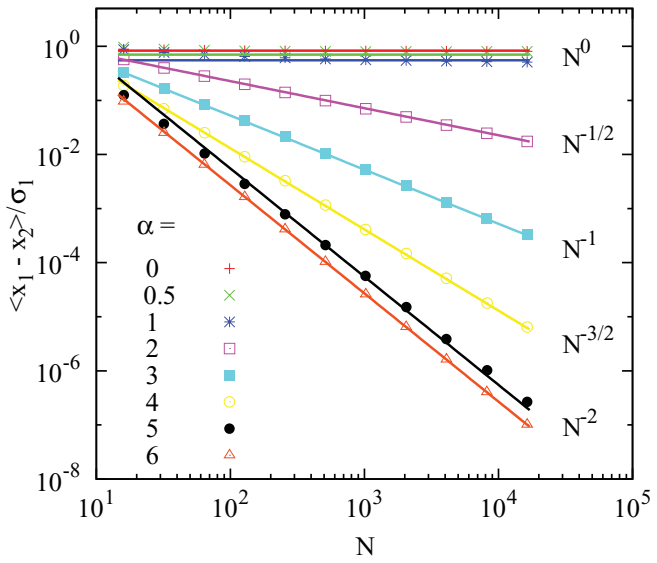

FIG. 3. (Color online) Difference between the $k = 1$ and 2 average maxima as a function of N for increasing α (top to bottom). The asymptotes are indicated on the right.

furthermore, the probability distribution $P(y)$ for the shifted maximum $y = x_1 - \langle x_1 \rangle$ is given by [38]

$$P(y) = [2e^{-y/2}K_1(2e^{-y/2})]', \tag{15}$$

where K_1 is the modified Bessel function. The agreement between $P(y)$ and the numerics in Fig. 2(c) is excellent.

As for the width of the distributions and the scaling of the gaps for $\alpha = 1$, we only have indications from simulations.

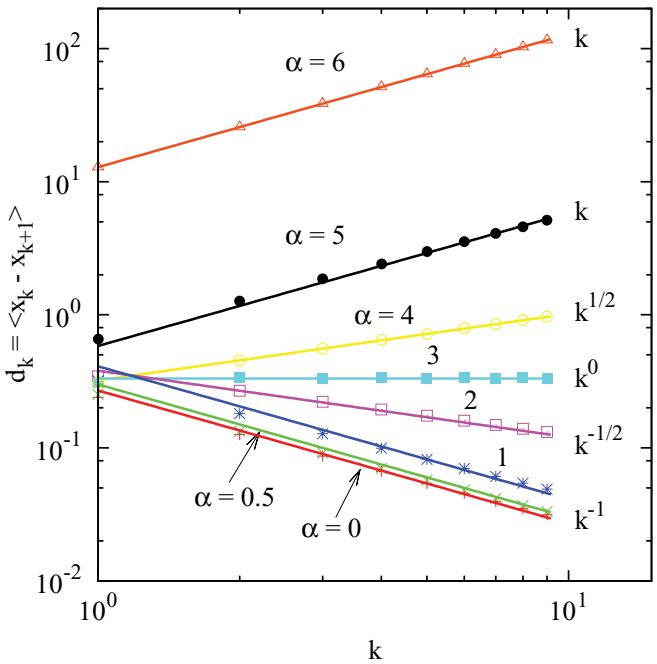

FIG. 4. (Color online) Average unscaled gap d_k for $\alpha = 0, 0.5, 1, \ldots, 6$ (bottom to top) obtained from simulations with $N = 16\,384$. The values of the limiting slopes are indicated at the end of the lines. The straight line fits are excellent except for $\alpha = 1$ and 5 where logarithmic corrections may be present.

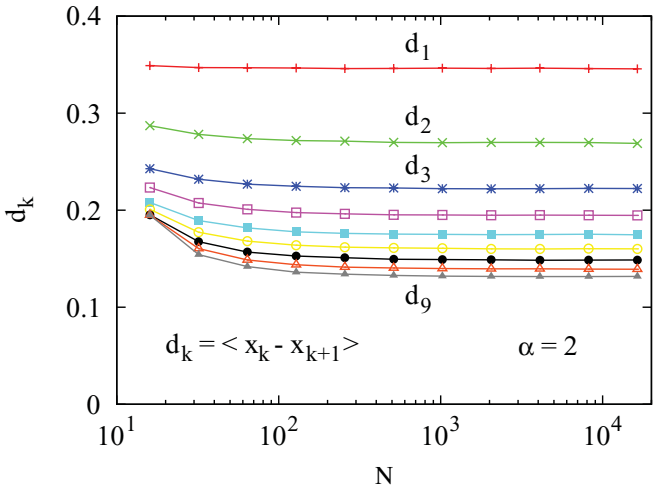

FIG. 5. (Color online) Unscaled gaps for $\alpha = 2$. The simulation results are for $N = 16, 32, \ldots, 16\,384$, and the lines are just guides for the eyes.

It appears that $\sigma_{k>1} \sim O(1)$, as for $k = 1$, and that the gaps d_k are also $O(1)$ for all examined k. Logarithmic crossovers prevent us from making any firm conclusions.

For $\alpha > 1$, the convergence to the limit distribution becomes a power law as seen in extensive simulations for general α [24] and also in the exact solution for $\alpha = 2$ [19,23]. Thus the convergence is faster, and the order statistics can be reliably investigated for $\alpha > 1$ (but not too close to $\alpha = 1$).

Figure 2(d) displays the $\alpha = 2$ results for $P_k(z)$, in which one can observe a new scaling regime. Namely, the histograms are barely distinguishable, i.e., the widths of the histograms σ_k are much larger than the gaps d_k. It is known [19] from the exact solution for $P_1(x)$ for $\alpha = 2$ that $\sigma_1 \sim \langle x_1 \rangle \sim N^{1/2}$. Thus our simulation results (see Fig. 3) indicating $\langle x_1 - x_2 \rangle / \sigma_1 \sim N^{-1/2}$ confirm that the first gap $d_1 = \langle x_1 - x_2 \rangle$ is indeed $\mathcal{O}(1)$. It then follows that there is no need for an N-dependent rescaling of the gap. The same result is obtained for all $d_k = \langle x_k - x_{k+1} \rangle$ as seen directly in Fig. 5, where the unscaled gaps for $\alpha = 2$ are plotted as functions of N.

Plots similar to those in Fig. 5 implying that $d_k \sim O(1)$ in the large N limit can be produced for any $1 < \alpha < 5$. The same conclusion can also be drawn from Fig. 3. Indeed, it is known [24] that $\sigma_1 \sim N^{(\alpha-1)/2}$, and since the asymptotes of the simulation results for d_k/σ_1 scale like $N^{-(\alpha-1)/2}$, one concludes that $d_k \sim O(1)$.

Once $d_k \sim O(1)$ is established, we can plot the unscaled d_k as a function of k. As can be seen in Fig. 4, the d_k display power-law scaling and the exponents for $\alpha = 2$, 3, and 4 are $-1/2, 0$, and $1/2$, respectively. These exponents, together with the -1 and $+1$ values (with possible logarithmic corrections) at $\alpha = 1$ and 5, suggest that in the interval $1 < \alpha < 5$

$$d_k \sim k^{(\alpha-3)/2}. \tag{16}$$

The above scaling can be derived from the phenomenological considerations embodied in Eqs. (12)–(14) which worked for

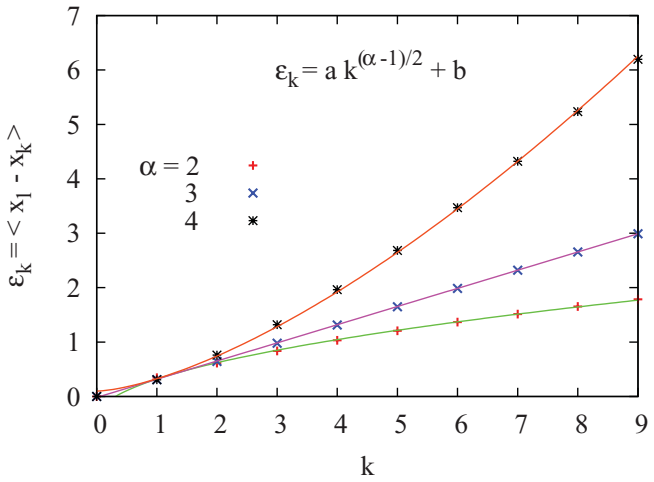

FIG. 6. (Color online) Spectra of the ordered values $\langle x_k \rangle$ measured from the largest value of the signal $\varepsilon_k = \langle x_1 - x_k \rangle$ for $\alpha = 2$, 3, and 4. Simulation results for $N = 16\,384$ are plotted together with two-parameter fits (solid lines) of the form $\varepsilon_k = ak^{(\alpha-1)/2} + b$, where a and b depend on α.

$\alpha < 1$. The starting point is the observation that the sum of d_k is of the order of x_1, and since $x_1 \sim N^{(\alpha-1)/2}$, we can write

$$\sum_{k=1}^{N/2} d_k \approx \langle x_1 \rangle \sim N^{(\alpha-1)/2}. \tag{17}$$

Assuming that the $d_k \sim k^\delta$ scaling is valid for large k of the order of N, we have

$$\sum_{k=1}^{N/2} k^\delta \approx N^{(\alpha-1)/2}, \tag{18}$$

and the above equality implies $d_k \sim k^{(\alpha-3)/2}$, as suggested by simulations.

The large k asymptote of the spectrum ε_k can now be obtained by integrating the $d_k \sim k^{(\alpha-3)/2}$ expression, yielding

$$\varepsilon_k \sim k^{(\alpha-1)/2}. \tag{19}$$

As can be seen from Fig. 6, fits of the form $\varepsilon_k = ak^{(\alpha-1)/2} + b$ are indeed excellent for $\alpha = 2$, 3, and 4. It should be noted, however, that the constant b is important for observing the exponent $(\alpha - 1)/2$. Naive straight-line fits on log-log plots of ε_k versus k yield poor estimates for the exponents since the constant b generates strong corrections to scaling in the range $0 < k < 10$ studied.

C. Large α regime ($5 \leqslant \alpha \leqslant \infty$)

The large α regime is special in that the second derivative of the signal becomes continuous for $\alpha \geqslant 5$. Then the largest local maximum $x_1 = x(t_1)$ and the values near it are expected to determine the order statistics, and this allows one to calculate the spectrum by expanding the signal around the maximum

$$x(t_1 + \Delta) = x_1 + \tfrac{1}{2}x''(t_1)\Delta^2 + O(\Delta^3), \tag{20}$$

where $\Delta = \tau, 2\tau, \ldots, (k-1)\tau$ are the positions of the second, third, ..., kth maximum, respectively. The justification for the above expansion comes from comparing the first and second terms on the right hand side of (20). The maximum value x_1 scales as $\langle x_1 \rangle \sim N^{(\alpha-1)/2}$, and the characteristic value of x'' can be estimated through $[\langle (x'')^2 \rangle]^{1/2}$. A straightforward calculation yields

$$[\langle (x'')^2 \rangle]^{1/2} \sim \langle |x''(t_1)| \rangle \sim N^{(\alpha-5)/2} \sim \langle x_1 \rangle N^{-2}, \tag{21}$$

showing that the second term is indeed much smaller than the first one [note that $\Delta \sim \tau = T/N \sim O(1)$ in the limit we are considering].

Using the expansion (20), the unscaled gap d_k can be written as

$$\langle x(t_1 + (k-1)\tau) - x(t_1 + k\tau) \rangle \approx \langle |x''(t_1)| \rangle \tau^2 k\,. \tag{22}$$

Next, the N dependence contained in $\langle |x''(t_1)| \rangle \tau^2 \sim N^{(\alpha-5)/2}$ is scaled out, and we obtain the gap as a function of k:

$$d_k \sim k, \tag{23}$$

and the corresponding spectrum then follows as

$$\varepsilon_k \sim k^2. \tag{24}$$

As can be seen in Fig. 4, the $\alpha = 5$ and 6 results for d_k are in excellent agreement with the $d_k \sim k$ scaling for small values of k as well.

It should be noted that the scaled first gap shown for $\alpha = 5$ and 6 on Fig. 3 can be also understood on the basis of the expansion [(20)–(22)]. Indeed, noting that $\langle x_1 \rangle \sim \sigma_1$, and using (21) with $k = 1$, we have

$$\frac{\langle x(t_1) - x(t_1 + \tau) \rangle}{\sigma_1} \sim \frac{\langle |x''(t_1)| \rangle}{\sigma_1} \sim \frac{1}{N^2}\,, \tag{25}$$

in agreement with the $\alpha \geqslant 5$ results on Fig. 3. The above result is exact in the $\alpha \to \infty$ limit where the signal is just a single mode $x(t) \sim x_1 \sin(2\pi t/T)$; thus the relationships $\langle x_1 \rangle \sim \sigma_1$ and $\langle |x''(t_1)| \rangle \sim \langle x_1 \rangle / N^2$ are trivially satisfied.

The simulations for $\alpha = 5$ and 6, together with the simplicity of the $\alpha \to \infty$ limit, suggest that the results (23)–(25) are valid for all $\alpha \geqslant 5$. The possible logarithmic corrections at the borderline point $\alpha = 5$ are outside the limits of our present simulations.

V. SUMMARY AND A CONNECTION TO THE DENSITY OF NEAR-EXTREME STATES

The results for the gap d_k and the spectra ε_k obtained in Sec. IV are summarized in columns 1–3 of Table I. As one can see from columns 2 and 3, there are three regimes and, furthermore, the gaps and the spectrum change with the noise properties (α) only in the $1 \leqslant \alpha < 5$ regime.

The above results for $1 < \alpha \leqslant \infty$ can be derived by considerations related to the density of near-extreme states. Namely, if we assume that the spectrum has a scaling form $\langle x_1 - x_k \rangle = \varepsilon_k \sim k^\beta$, then the density of states near the extreme is $\rho(\delta x) \sim (\delta x)^{1/\beta}/\delta x \sim (\delta x)^{1/\beta - 1}$; thus knowledge of the small argument asymptote $\rho(\delta x) \sim (\delta x)^\gamma$ allows one to deduce the exponent $\beta = 1/(\gamma + 1)$.

The density of near-extreme states $\rho(\delta x)$ was first investigated for i.i.d. variables by Sabhapandit and Majumdar [25]. Later, it was shown by Burkhardt *et al.* [26] that $\rho(\delta x)$ can be obtained for periodic signals as the distribution $\Phi_I(x)$ of

TABLE I. Gaps d_k and spectra ε_k in the order statistics of $1/f^\alpha$ signals as obtained in simulations and suggested by scaling arguments. The fourth column displays the one-dimensional potential $V(x)$ in which the quantum mechanical motion of a particle generates energy spectra with the same scaling properties.

α	d_k	ε_k	$V(x)$
$0 \leqslant \alpha < 1$	k^{-1}	$\ln k$	$\ln \lvert x \rvert$
$1 \leqslant \alpha < 5$	$k^{(\alpha-3)/2}$	$k^{(\alpha-1)/2}$	$\lvert x \rvert^{2(\alpha-1)/(5-\alpha)}$
$5 \leqslant \alpha \leqslant \infty$	k	k^2	$\lvert x \rvert^{\infty}$

the maximum with respect to the initial value $x = \max_t x(t) - x(0)$. The distribution $\Phi_I(x)$ for periodic $1/f^\alpha$ signals has been investigated by simulations as well as through exact solutions for the particular cases of $\alpha = 2$, 4, and ∞ [26]. The small argument behavior of Φ_I was indeed found to have a power-law form $\Phi_I(\delta x) \sim (\delta x)^\gamma$ with [see Eq. (65) in Ref. [26]]

$$\gamma(\alpha) = \begin{cases} \frac{3-\alpha}{\alpha-1}, & \alpha < 5 \\ -\frac{1}{2}, & \alpha \geqslant 5. \end{cases} \tag{26}$$

The scaling exponents of the spectra following from the above expression [$\beta = 1/(\gamma + 1)$] are equal to those in Table I for $1 < \alpha \leqslant \infty$, thus reinforcing our earlier conclusions. Since the exponents in (26) are exact for $\alpha = 2$, 4, and ∞, we can conclude that the corresponding $\beta(\alpha)$ exponents depend on the validity of the $\varepsilon_k \sim k^\beta$ scaling.

VI. COMPARING WITH QUANTUM SPECTRA

We shall now compare the order statistics spectra to the energy spectra of quantum mechanical systems in the quasiclassical limit. The reason for this comparison, apart from its entertaining aspects, is that the discrete quantum mechanical spectra may also be considered as an order statistics spectra.

Let us consider a particle of mass m which moves in a potential

$$V(x) = g|x|^\theta, \tag{27}$$

where $g > 0$ is the coupling constant. The simplest way to calculate the quasiclassical limit of the spectra is to use dimensional analysis combined with the observation that, in the large quantum-number limit ($k \to \infty$), the quantization condition ($\int p dq = kh$) forces h and k to appear in the combination hk. This means that the k dependence of the spectra is determined by its h dependence. Since the energy is uniquely determined by the dimensions of m, q, and h, one obtains

$$E_k \sim (hk)^{\frac{2\theta}{\theta+2}}. \tag{28}$$

Comparing the above result with column 3 in Table I, one can see that there is a mapping between the quantum mechanical and the order statistics exponents. The large-α regime ($5 \leqslant \alpha \leqslant \infty$) corresponds to the infinite square-well potential ($\theta = \infty$), while θ changes monotonically from 0 to ∞ in the nontrivial regime ($1 < \alpha < 5$), and the correspondence is given by

$$\theta = \frac{2(\alpha - 1)}{5 - \alpha}. \tag{29}$$

The above considerations cannot be applied for the remaining $0 \leqslant \alpha \leqslant 1$ range, but the order statistics spectrum $\varepsilon_k \sim \ln k$ suggests that the corresponding potential is of the form $V(x) \sim \ln|x|$.

We would like to emphasize that it is not obvious that the mapping between the exponents has any physical content. Nevertheless, it is intriguing to ask whether there is a *quasiclassical* extreme value question whose answer is the quantum mechanical spectra.

VII. FINAL REMARKS

Studying the order statistics in $1/f^\alpha$ signals, we found three scaling regimes as summarized in Table I. In the case of weakly correlated stationary signals ($0 < \alpha < 1$), the i.i.d. result ($d_k \sim k^{-1}$) applies, while for strongly correlated signals ($1 \leqslant \alpha \leqslant \infty$), the scaling depends on whether the signal is twice differentiable ($\alpha \geqslant 5$) or not ($1 \leqslant \alpha < 5$). In the former case, order statistics ($d_k \sim k$) follows from expanding the signal around the maximum. In the latter case, the observed scaling ($d_k \sim k^{(\alpha-3)/2}$) is derived using a phenomenological argument (exact for i.i.d. variables), namely, that the sum over d_k scales in the same way as $\langle x_1 \rangle$. Meanwhile, the spectrum ε_k is essentially obtained by integrating d_k. The same scaling picture was also obtained by relating order statistics to the density of near-extreme states studied in previous works.

It is clear that investigating the order statistics of correlated systems will help in characterizing and understanding extreme events in more detail. It is also clear, however, that the results for $1/f^\alpha$ signals have a restricted range of applicability, and much more is needed to advance our understanding of the effects of various correlations. Nevertheless, there are phenomena where $1/f^\alpha$ type fluctuations do emerge, the extremes are important, and, consequently, our results may be utilized. A possible application is to climate records (temperature, precipitation, etc.) which often display, e.g., clustering of extreme events, and the power spectrum of the fluctuations appears to be of the $1/f^\alpha$ type [9,42].

ACKNOWLEDGMENTS

This research has been supported by the Hungarian Academy of Sciences through OTKA Grants No. K 68109 and No. NK 72037. We would like to thank T. Burkhardt, S. N. Evans, G. Györgyi, and M. Z. Rácz for helpful discussions.

[1] R. A. Fisher and L. H. C. Tippett, Proc. Cambridge Philos. Soc. **24**, 180 (1928).

[2] J. Galambos, *The Asymptotic Theory of Extreme Value Statistics* (Wiley, New York, 1978).

[3] L. de Haan and A. Ferreira, *Extreme Value Theory: An Introduction* (Springer, New York, 2006).
[4] E. J. Gumbel, *Statistics of Extremes* (Dover Publications, Inc., New York, 2004).
[5] W. Weibull, Trans. ASME, J. Appl. Mech. **18**, 293 (1951).
[6] P. Embrecht, C. Klüppelberg, and T. Mikosch, *Modelling Extremal Events for Insurance and Finance* (Springer, Berlin, 1997).
[7] R. W. Katz, M. B. Parlange, and P. Naveau, Adv. Water Resour. **25**, 1287 (2002).
[8] H. v. Storch and F. W. Zwiers, *Statistical Analysis in Climate Research* (Cambridge University Press, Cambridge, 2002).
[9] J. F. Eichner, J. W. Kantelhardt, A. Bunde, and S. Havlin, Phys. Rev. E **73**, 016130 (2006).
[10] B. Gutenberg and C. F. Richter, Bull. Seismol. Soc. Am. **34**, 185 (1944).
[11] M. J. Geller and P. J. E. Peebles, Astrophys. J. **206**, 939 (1976).
[12] Y.-T. Lin, J. P. Ostriker, and C. J. Miller, Astrophys. J. **715**, 1486 (2010).
[13] J.-P. Bouchaud and M. Mézard, J. Phys. A **30**, 7997 (1997).
[14] P. L. Krapivsky and S. N. Majumdar, Phys. Rev. Lett. **85**, 5492 (2000).
[15] M. Z. Bazant, Phys. Rev. E **62**, 1660 (2000).
[16] A. Lakshminarayan, S. Tomsovic, O. Bohigas, and S. N. Majumdar, Phys. Rev. Lett. **100**, 044103 (2008).
[17] S. Raychaudhuri, M. Cranston, C. Przybyla, and Y. Shapir, Phys. Rev. Lett. **87**, 136101 (2001).
[18] G. Györgyi, P. C. W. Holdsworth, B. Portelli, and Z. Rácz, Phys. Rev. E **68**, 056116 (2003).
[19] S. N. Majumdar and A. Comtet, Phys. Rev. Lett. **92**, 225501 (2004).
[20] H. Guclu and G. Korniss, Phys. Rev. E **69**, 065104(R) (2004).
[21] C. J. Bolech and A. Rosso, Phys. Rev. Lett. **93**, 125701 (2004).
[22] D.-S. Lee, Phys. Rev. Lett. **95**, 150601 (2005).
[23] G. Schehr and S. N. Majumdar, Phys. Rev. E **73**, 056103 (2006).
[24] G. Györgyi, N. R. Moloney, K. Ozogány, and Z. Rácz, Phys. Rev. E **75**, 021123 (2007).
[25] S. Sabhapandit and S. N. Majumdar, Phys. Rev. Lett. **98**, 140201 (2007).
[26] T. W. Burkhardt, G. Györgyi, N. R. Moloney, and Z. Rácz, Phys. Rev. E **76**, 041119 (2007).
[27] S. N. Majumdar and A. J. Bray, Phys. Rev. Lett. **86**, 3700 (2001).
[28] S. Redner, *A Guide to First-Passage Processes* (Cambridge University Press, Cambridge, 2001).
[29] M. R. Leadbetter, G. Lindgren, and H. Rootzen, *Extremes and Related Properties of Random Sequences and Processes* (Springer-Verlag, New York, 1982).
[30] S. N. Majumdar, Current Science **77**, 370 (1999).
[31] S. Redner and M. R. Petersen, Phys. Rev. E **74**, 061114 (2006).
[32] G. Wergen and J. Krug, Europhys. Lett. **92** , 30008 (2010).
[33] G. Wergen, M. Bogner, and J. Krug, Phys. Rev. E **83**, 051109 (2011).
[34] J. Pickands, Ann. Stat. **3**, 119 (1975).
[35] L. Dobos and I. Csabai, MNRAS **414**, 1862 (2011).
[36] S. Tremaine and D. Richstone, Astrophys. J. **212**, 311 (1977).
[37] E. Brunet and B. Derrida, Europhys. Lett. **87**, 60010 (2009).
[38] Y. V. Fyodorov, P. Le Doussal, and A. Rosso, J. Stat. Mech.: Theory Exp. (2009), P10005.
[39] T. Antal, M. Droz, G. Györgyi, and Z. Rácz, Phys. Rev. E **65**, 046140 (2002).
[40] G. Györgyi, N. R. Moloney, K. Ozogány, and Z. Rácz, Phys. Rev. Lett. **100**, 210601 (2008).
[41] S. M. Berman, Ann. Math. Stat. **33**, 502 (1964).
[42] J. F. Eichner, E. Koscielny-Bunde, A. Bunde, S. Havlin, and H.-J. Schellnhuber, Phys. Rev. E **68**, 046133 (2003).